AD_____

Award Number: W81XWH-10-1-0026

TITLE: P53 Suppression of Homologous Recombination and Tumorigenesis

PRINCIPAL INVESTIGATOR: Bijal Karia, B.S.

CONTRACTING ORGANIZATION: Texas, University of, Health Science Center at San Antonio
San Antonio, TX 78229

REPORT DATE: January 2013

TYPE OF REPORT: Annual Summary

PREPARED FOR: U.S. Army Medical Research and Materiel Command
Fort Detrick, Maryland 21702-5012

REPORT DOCUMENTATION PAGE

Form Approved
OMB No. 0704-0188

1. REPORT DATE	2. REPORT TYPE	3. DATES COVERED
January 2013	Annual Summary	1 January 2012 - 31 December 2012

4. TITLE AND SUBTITLE

P53 Suppression of Homologous Recombination and Tumorigenesis

5a. CONTRACT NUMBER

5b. GRANT NUMBER
W81XWH-10-1-0026

5c. PROGRAM ELEMENT NUMBER

6. AUTHOR(S)

Bijal Karia

E-Mail: BIJALKARIA79@GMAIL.COM

5d. PROJECT NUMBER

5e. TASK NUMBER

5f. WORK UNIT NUMBER

7. PERFORMING ORGANIZATION NAME(S) AND ADDRESS(ES)

Texas, University of, Health Science Center at San Antonio
San Antonio, TX 78229

8. PERFORMING ORGANIZATION REPORT NUMBER

9. SPONSORING / MONITORING AGENCY NAME(S) AND ADDRESS(ES)
U.S. Army Medical Research and Materiel Command
Fort Detrick, Maryland 21702-5012

10. SPONSOR/MONITOR'S ACRONYM(S)

11. SPONSOR/MONITOR'S REPORT NUMBER(S)

12. DISTRIBUTION / AVAILABILITY STATEMENT
Approved for Public Release; Distribution Unlimited

13. SUPPLEMENTARY NOTES

14. ABSTRACT

Maintaining genomic stability is critical for organismal fitness. Consequently, the absence of tumor suppressor gene activity, such as p53, results in increased genomic instability and increased cancer predisposition. Homologous recombination (HR), as measured by the in vivo pun assay, is a DNA repair mechanism that our laboratory uses to measure genomic instability. We compared eyespot frequency in normal wild type mice, mice that are absent in p53 protein (null) and those that have the hotspot mutations R172H and R172P (equivalent to R175 in human breast cancer). Previously, we have shown that in the absence of p53 the normal frequency of spontaneous HR is significantly elevated. However, the mechanism by which p53 suppresses HR is unclear. The p53 R172P mutant mice retains limited transcriptional functionality (regulating cell cycle genes but not apoptotic genes) while the p53 R172H mutant mice lack any transcriptional activity but retain some protein: protein interaction capability. We observed significantly increased HR frequency in the p53 R172H mutant versus the p53 R172P mutant mice. This suggests that p53 regulation of cell cycle genes but not apoptotic genes may be responsible for its ability to suppress HR frequency. Also, the loss of key protein: protein interactions may have contributed to this suppression. It has been previously reported that p53 R172H mutant mice come down with early aggressive tumors compared to the p53 R172P mutant mice. This correlates with the increased HR frequency we observed in the R172H mutant mice implicating p53 suppression of genomic instability as a major mechanism for p53 tumor suppression. This work provides novel insight into the mechanism of cancer development in the absence or mutation of p53 and the mechanism of p53 control of HR in an in vivo system. p53 is often a targeted therapy and further insight into the function of p53 in DNA repair pathways can be vital to finding novel points of targeted therapy. Our data will add insight to the important paradigm of genomic instability and its relation to breast cancer etiology.

15. SUBJECT TERMS
HOMOLOGOUS RECOMBINATION, P53 HOTSPOT MUTATIONS, BREAST CANCER, GENOMIC INSTABILITY, TUMORIGENESIS

16. SECURITY CLASSIFICATION OF:			17. LIMITATION OF ABSTRACT	18. NUMBER OF PAGES	19a. NAME OF RESPONSIBLE PERSON
a. REPORT	b. ABSTRACT	c. THIS PAGE			USAMRMC
U	U	U	UU	41	19b. TELEPHONE NUMBER *(include area code)*

Table of Contents

Introduction

The purpose of this project is to determine the mechanism for how the tumor suppressor, p53, suppresses homologous recombination. P53 is implicated in 50% of all human cancers and inactivated in some form in 100% of human cancers. Homologous recombination (HR) is an error proof repair mechanism that is able to repair any type of DNA lesion with high fidelity. However, when the HR machinery uses an incorrect template for repair large deletions in the genome can occur leading to a predisposition for cancer. P53 has been implicated in suppressing homologous recombination in order to maintain genomic stability, however the mechanism is still unknown. In the first year of this grant huge strides have been made in the numbers of mice breed and relevant cells collected for the purposes of experiments outlined in the aims below. The PI has optimized the pun assay and mouse husbandry in the first year of this grant and has collected data during the second year of the grant period. The second year accomplishments included three middle author publications due to the PI's knowledge, and expertise in various areas including p53 mutation, DNA repair and cell cycle function. The PI also attended two conferences in the preceding year where she presented a poster and had several committee meetings to evaluate the work progress. In the current report period, the PI completed work for specific aims listed in the initial proposal and is in the process of completing two first author manuscripts and writing her dissertation. Experiments and final committee meeting have been completed. The PI is currently writing and preparing for her defense to be held in April 2013.

Body

P53 is a potent tumor suppressor that shields the genome from daily interrogations of endogenous and exogenous damage, most importantly through its ability to arrest the cell cycle. In response to damage, p53 up regulates transcription of p21 leading to G1 arrest, which allows adequate time for repair of lesions before entering S phase (1, 2). Furthermore, p53 has been linked to G2/M arrest through multiple overlapping p53-dependent and p53-independent pathways that inhibit cdc2 (3). As a final resort if the damage is severe enough p53 has been shown to induce apoptosis in certain situations (2, 4).

P53 has also been linked to various DNA repair pathways such as non-homologous end joining (NHEJ) and homologous recombination (HR). Homologous recombination is a high fidelity DNA repair mechanism that can repair almost any type of DNA lesion when in correct equilibrium. When this delicate balance is disrupted as seen in *Blm* null cells resulting in hyperrecombination or hyporecombination in *Brca1* null cells the ensuing result is genomic instability (5).

It has been reported previously that p53 down regulates spontaneous homologous recombination in chromosomally integrating plasmid substrate models. Bertrand *et al*. using a plasmid-based system with PJS3-10 (mouse L cell lines) overexpressed the mutant $p53^{175\ (Arg>His)}$, which showed a 5-20 fold increase in spontaneous recombination compared to wild type control cells. Further analysis showed that the effect of the p53 mutation acted on both rad51 dependent gene conversion events and deletion events (6).

Willers *et al*. also showed an increase in recombination frequency in a temperature sensitive p53 mutant (Ala135 to Val) using a plasmid substrate that stably integrated into p53 null mouse embryonic fibroblasts (MEFs). This study further established the uncoupling of p53's function in suppressing HR and its role as a cell cycle checkpoint protein (7).

The Wiesmuller lab has explored the role of p53 in HR using a rare cutting endonuclease ISCE-1 in breast cancer cells with varying p53 mutations. This study used a DSB repair assay to show that some p53 mutants retain partial ability to repair double strand breaks by repressing aberrant HR and less infrequently through NHEJ and SSA(8).

P53 is mutated in 50% of all human cancers and most likely inactivated by some other mechanism in the other 50%. Patients with Li Fraumeni syndrome suffer from a germ line mutation in p53 and subsequently endure an early onset of cancer. Mouse models have been created to recapitulate this phenomenon and are surprisingly viable. 80% of P53 null mice come down with lymphomas within 6 months and the rest suffer from sarcomas. MEFs from these mice show aneuploidy, allelic loss and gene amplification. Most of these germline mutations are missense mutations occurring in the DNA binding domain of p53. One such mutant is the p53-R172P and p53-

R172H mouse model (9). The p53-R172P mouse is able to induce partial cell cycle arrest in response to DNA damage but is defective in promoting apoptosis. Mice homozygous for this mutation escape the early onset of lymphomas that is typical for p53 null mice, however these mice eventually do succumb to tumors that have a normal diploid number of chromosomes in contrast to p53 null tumors. The p53-R172H mouse shows an inability to transactivate p53 target genes as well as a defect in apoptosis induction (10). A majority of mice homozygous for p53-R172H developed lymphomas similar to p53 null mice with a smaller percent developing sarcomas. P53-R172H heterozygous mice developed sarcomas and a surprising number of osteosarcomas and carcinomas that metastasized, which were not seen in p53 heterozygous mice (9). Interestingly, the p53-R172H tumors showed a high level of aneuploidy similar to p53 null mice but unlike p53-R172P mice. Given this we sought to look at the HR frequency of these two mutants to determine if there is a difference in in the ability to suppress HR similar to WT given the different functionalities of these to mutants. HR is measure of genomic instability, even though it can fix any type of genotoxic lesion, when used incorrectly it can cause large deletions and lesions in the genome. Using the in vivo pun assay we have seen an increase in HR frequency in many mouse models of the DNA damage repair pathway. HR frequency is increased in BLM null, p53 null and parp null mice and decreased in Brca1 and Brca2 null animals (5, and unpublished work).

Given the power of this assay here we used the *in vivo* p^{un} assay to determine the consequence of HR suppression in two breast cancer hotspot p53 mutant mouse models with differing loss of function. The p53-R172P mice, which are defective in their ability to induce apoptosis but are able to induce cell cycle genes, retained the ability to suppress HR similar to wild type p53 animals. The more aggressive p53-R172H mouse showed increase HR similar to p53 null mice, which do not produce any p53 protein at all.

Specific Aim 1: Determine whether p53 mutants R172P and R172H suppress spontaneous levels of homologous recombination the same as wild-type p53.

In the first year of the training grant great effort was put forth to establish a robust breeding colony of R172P, R172H, Wild type and p53 null mice in order to have sufficient numbers of animals to perform the in vivo pun assay in the second year of training.

Mouse Strains and Breeding Cohorts

Mice heterozygous for the point mutants $p53^{R172P}$ and $p53^{R172H}$ (C57BL/6 genetic background) were kindly provided by Dr. G. Lozano (M.D. Anderson). Two additional crosses to C57BL/6 $p^{un/un}$ mice (purchased from the Jackson Laboratory, Bar Harbor, ME). Mice heterozygous for a targeted

null allele of p53 (herein referred to as neo) were previously crossed into a C57BL/6J $p^{un}/^{un}$ genetic background (Aubrecht et al. 1999).

Breeding cohorts of $p53^{R172P/+}$ $p^{un/un}$, $p53^{R172H/+}$ $p^{un/un}$ and $p53^{neo/+}$ $p^{un/un}$ were established and maintained by intercrossing heterozygous mice in each respective cohort to produce the desired experimental mice ($p53^{R172P/R172P}$ $p^{un/un}$, $p53^{R172H/R172H}$ $p^{un/un,}$ $p53^{neo/neo}$ $p^{un/un}$) along with littermate controls ($p53^{R172P/+}$ $p^{un/un}$, $p53^{R172H/+}$ $p^{un/un,}$ $p53^{neo/+}$ $p^{un/un}$, $p53^{+/+}$ $p^{un/un}$). Animal studies were carried out in accordance with UTHSCSA and IACUC policies as outlined in protocol 05054-34-01-A.

Genotyping

The $p53^{R172P}$, $p53^{R172H}$ and $p53^{neo}$ genotypes were determined by polymerase chain reaction (PCR) analysis as previously described (Liu et al. 2004, Aubrecht et al. 1999). The $p^{un/un}$ genotype was identified by the phenotypic dilute (grey) coat color.

p^{un} Eyespot HR Assay

Heterozygous mice from the breeding cohorts established in the first year: $p53^{R172P/+}$ $p^{un/un}$, $p53^{R172H/+}$ $p^{un/un}$ and $p53^{neo/+}$ $p^{un/un}$ mice were intercrossed in each respective cohort to produce the desired experimental mice ($p53^{R172P/R172P}$, $p53^{R172H/R172H}$, $p53^{neo/neo}$) along with littermate controls ($p53^{R172P/+}$, $p53^{R172H/+}$, $p53^{neo/+}$, $p53^{+/+}$). Mice were then sacrificed at weaning age and their eyes harvested and dissected to expose the retinal pigment epithelium (RPE) as previously described (12). Briefly, each RPE whole mount was digitally photographed and analyzed for eyespots using a Zeiss Lumar version 12 stereomicroscope, Zeiss AxioVision MRm camera, and Zeiss AxioVision 4.6 software (Thornwood, NY) as described previously (13, appendix). The criteria for what constitutes an eyespot was previously defined in bishop *et al*. as being a pigmented cell that is separated by 2 other pigmented cells (12). Next, the RPE images were uploaded into Adobe Photoshop and the edge of the RPE was delineated using the ellipse tool and free transform path function. Two measurements were made (i) a frequency of eyespots (HR events) per RPE, and (ii) distribution of the eyespots within the RPE (their position) reflecting the developmental time at which the eyespots were produced.

Statistics

The Kruskal-Wallis test (non-parametric, one-way analysis of variance for multiple group comparison) followed by the Dunn's Multiple Comparison test was performed using GraphPad Prism (La Jolla, CA).

The recessive R172P mutation retains the ability to suppress HR in vivo

P53 is a potent tumor suppressor and plays an important role in protecting the genome from endogenous and exogenous damage. HR is the only DNA repair mechanism that is able to mend any lesion with high fidelity when it is working correctly. P53, although not a direct player in HR, helps the cell decide whether HR will be the best route to take. The R172P point mutation in p53 results in a mouse that is unable to transcribe apoptotic genes but is still able to arrest the cell cycle and retains most of its protein: protein interactions.

The frequency of p^{un} reversion was determined in $p53^{R172P/R172P}$ $p^{un/un}$ mice using the *in vivo* p^{un} assay (Table 1 and Figure 1). There was no significant increase in the number of eyespots compared to wild type. Suggesting that p53-R172P mutant mice retain the ability to suppress homologous recombination similar to wild type mice. The inability to transcribe apoptotic genes in this particular mutant had no impact on its ability to suppress HR, suggesting that the mechanism for p53 involvement in HR may be cell cycle mediated or through protein: protein interactions.

The aggressive R172H mutant mice show increased HR frequency similar to p53 null mice in vivo

The R172H point mutation results in a protein being formed but it is unable to bind and transcribe any of the p53 target genes. Also many of the normal protein: protein interactions have also been disrupted. The p53- R172H mutation is more detrimental than the R172P mutation in that the former mice have an earlier onset of tumors and a higher incidence of metastatic tumors in the heterozygous genotype.

The frequency of p^{un} reversion events in the p53-R172H mouse was significantly higher than the wild type controls and p53-R172P mutant mice ($p < .001$) (Table 1 and figure 1). Interestingly, the p^{un} reversion frequency was similar to that of a p53 null animal that produces no p53 protein at all (~ 10 eyespots).

	TOTAL			AVERAGE					
Genotype	RPE	Eyespots	Cells	Eyespots per RPE	SD	Cells per RPE	SD	Spot Size	SD
Wildtype	41	153	441	3.7	2.3	10.7	11	2.8	3.5
$p53^{neo/neo}$ $p^{un/un}$	22	258	680	11.7	6.6	31	27	2.6	3.4
$p53^{R172P/R172P}$ $p^{un/un}$	29	118	323	4.1	2.6	11.5	15.4	2.7	5.2
$p53^{R172H/R172H}$ $p^{un/un}$	35	340	742	9.7	4.6	21.2	13.9	2.2	2.5

Table 1: Summary of RPE analyzed and pun reversion frequency by p53 genotype

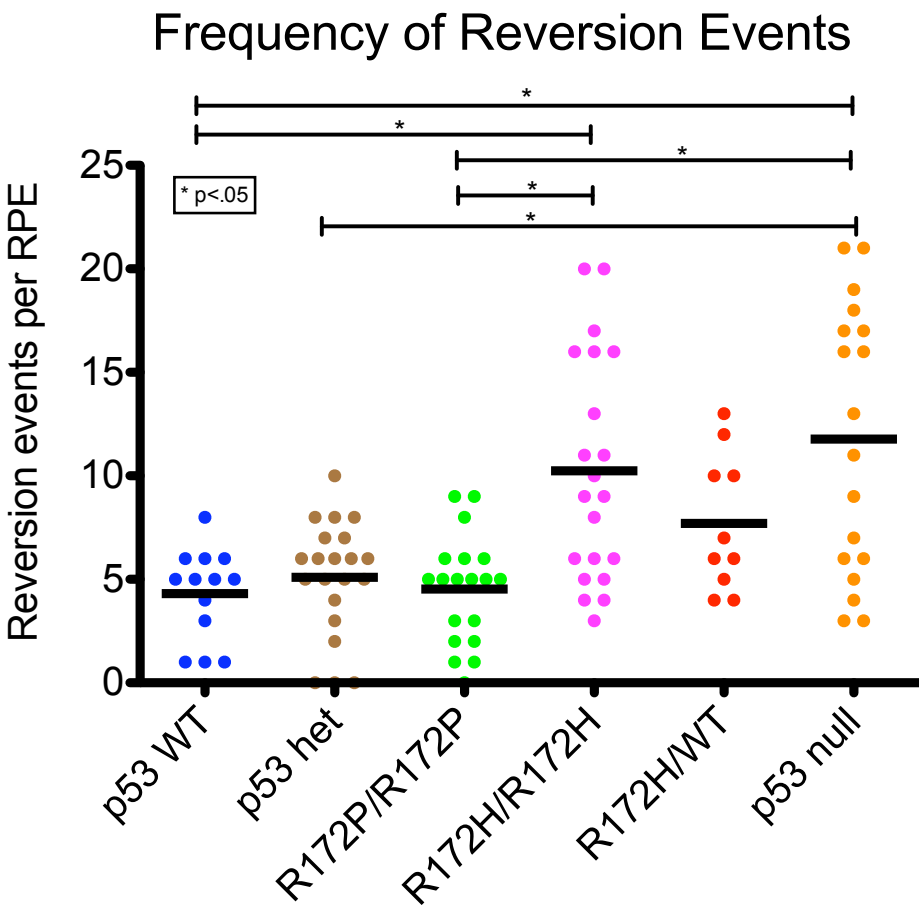

Figure 1. The frequency of eyespots was determined using the pun assay. The data indicates that p53 R172P mutant mice retained the ability to suppress HR similar to WT p53 mice. However, p53 R172H mutant mice showed increased HR frequency similar to p53 null mice. $p<0.001$.

A more sophisticated measurement that can be made using the pun eye assay is the relative position of the eyespot on the RPE. We performed this analysis (Figure 2.) and were surprised to see that there was a difference in these results in comparison to previous findings by the PI's mentor. Previous work showed that p53 null animals showed an increased number of eyespots closer to the optic nerve (towards the center) indicating a time in early development ~E8. This was not seen in the current work and can be explained by the difference in where the cutoff is made in the edge of the RPE. The current work shows a larger portion of the RPE whereas the previous work was a tighter circle around the RPE. This would lead to more spots being counted on the edge of the RPE that what was previously reported (14). There is no significant difference between the p53 mutants and WT in terms of their positional distribution on the RPE. Thus these events are not time in development as was previously reported for p53 null mice (14).

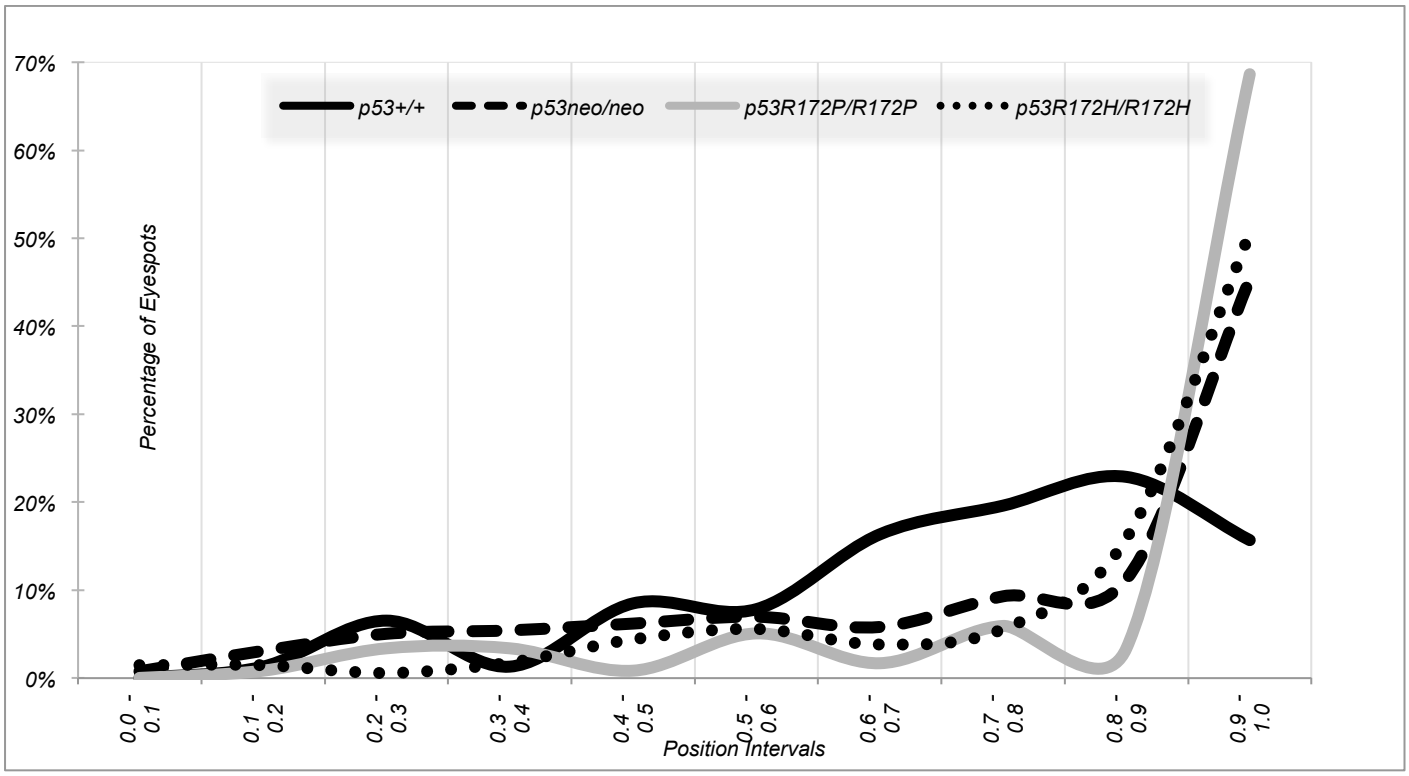

Figure 2. The relative position distribution of eyespots was determined using the pun assay. $P<0.05$

Because these mouse models are not a true separation of function (none exist in mouse models) we needed to further explore the relationship between p53's transcription factor capability and protein: protein interaction capability to delineate which have been disrupted between the R172P and R172H mutant to cause the change in HR suppression.

The microarray analysis showed few relevant genes that were different between R172P and R172H p53 mutants

We performed microarray analysis to determine transactivation differences between R172P and R172H mutant mice. We used an Agilent whole mouse array on mouse embryonic fibroblasts from each p53 mutant. We focused our analysis on homologous recombination, cell cycle, and apoptotic genes that may be dysregulated between the two mutants (Figure 3).

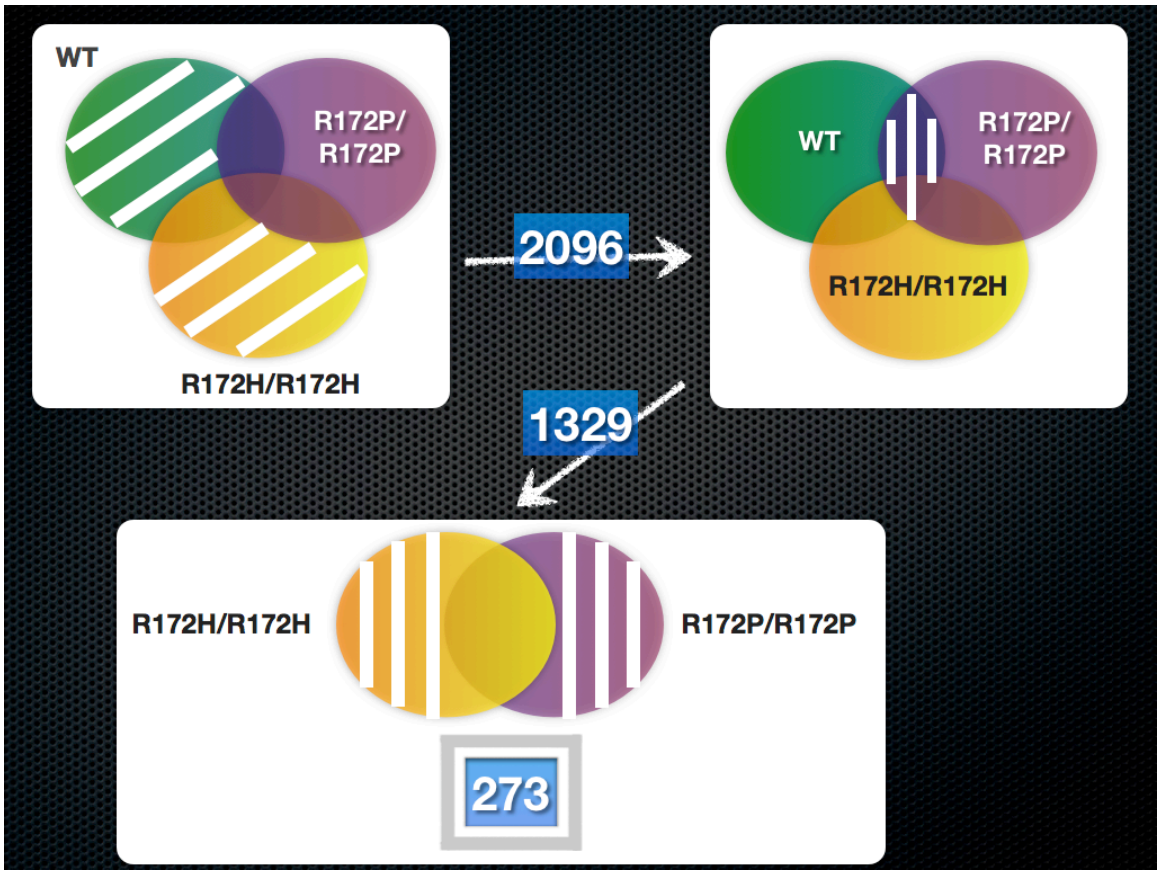

Figure 3: Schematic of the strategy used to narrow down the gene hit list. We compared 2 p53 mutants with WT resulting in 2096 genes. This comparison was then further narrowed by taking out all those genes that overlapped between WT and R172P (HR frequency was not different between these genotypes) resulting in a final gene list of 273 genes that were different between R172H and R172P.

We did not find any relevant genes that were differentially expressed between the two mutants. We compared our hit list of 273 genes to known p53 target genes and found no overlapping genes (Appendix 1). We thus attempted to see if there were indirect genes that may be in common with our hit list and known p53 target genes. Using an in-house analysis software created by Mark Doderer from the GCCRI bioinformatics core we narrowed our list further to 9 genes that might be relevant to the difference in homologous recombination we see between the p53 mutants (Figure 4). Of these 9 genes two are relevant in HR repair- Rad52 and XRCC3 (codes for rad51 protein). We will next validate these two hits in CO-IP and RT-PCR experiments. We are currently optimizing Rad51 and Rad52 antibodies in western blot and have attempted several rounds of Coimmunoprecipitation experiments with little success. We will attempt to tag these proteins with FLAG or HA in order to

have enough protein pulled down to determine if an interaction is broken between mutant p53 and rad51/52. The problem is that p53 is expressed in very low levels in an undamaged cell therefore tagging p53 or over expressing p53 will allow us to detect the p53 protein and bound proteins.

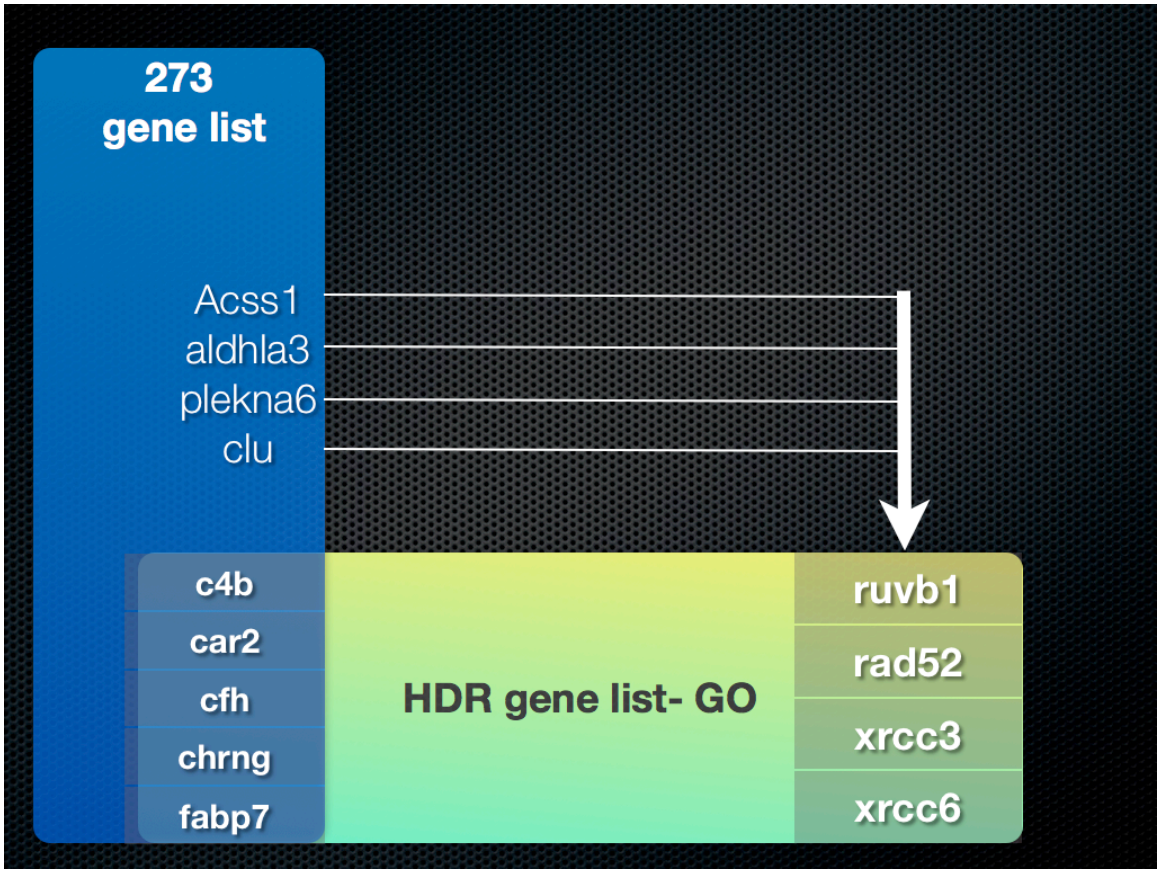

Figure 4: Using Sidekick (created by Mark Doderer) we compared our gene list of 273 genes with homologous directed repair genes (based on Gene Ontology). This comparison resulted in 9 genes.

Protein-Protein interaction analysis proves to be difficult in undamaged cells due to very low p53 protein expression.

To determine if a protein: protein interactions are disrupted in p53 mutant cells causing the loss of suppression of HR we attempted to perform co-immunoprecipitation analysis on WT, R172p, R172H and neo MEFs. We focused on proteins that were relevant in HR such as BRCA/2, Rad51, RPA, 53bp1 and bcl2 to determine if there are broken interactions in the R172H mutation and not in the R172P mutant. We have come across the problem of too little p53 protein being pulled down to determine an interaction or lack of one. P53 is expressed in very low levels in the cell when it is in a

spontaneous undamaged state. In order to have enough protein pull down to determine interactions we will need to damage the cells (IR) or over express and tag p53 (FLAG or HA etc.). We are currently working in collaboration with a biochemistry lab to optimize this assay.

Specific Aim 2: Determine the influence of the two p53 mutant mice on BER and NER activity as a mechanism by which p53 suppresses homologous recombination.

The NER and BER assays are currently being optimized in the lab. All resources and relevant p53 mutant cells have been collected. This aim and other alternate mechanisms will be the focus in the remaining time of this grant.

We are currently looking at alternative mechanisms that may play a role in the ability of p53 to suppress HR and guard the genome. A manuscript regarding this data is in preparation and will be submitted with final report.

Specific Aim 3. Determine whether either of the p53 mutants can alter the damage induced HRR response

In the first year of the grant sufficient mice were generated for *in vivo* pun analysis for spontaneous and damage induced experiments. In the second year of this grant we performed timed matings to intercross heterozygous mice in each cohort $p53^{R172P/+}$ $p^{un/un}$, $p53^{R172H/+}$ $p^{un/un}$ and $p53^{neo/+}$ $p^{un/un}$. The pregnant dams were then exposed to 1Gy of X-ray at E12.5 (Table 2). The pun reversion assay was performed as described in specific aim 1.

The results show that the HR is increased following irradiation in p53 WT mice as expected and reported elsewhere. Upon damage p53 stabilizes through post translational modifications and is then able to respond to damage via by acting through the DNA damage response pathway. We see this robust increase in HR in the R172P mutant as well but not in the R172H mutant. This suggests that the R172P mutant still retains the functionality needed to initiate a proper p53 response something the R172H mutant has lost. The R172H mutant behaves similarly to a mouse with not p53 protein (p53 null) in that the response is similar to what is seen in the spontaneous situation no further increase in HR is seen. We are in the process of weaning the pups from exposed dams and harvesting their eyes to further assess the frequency of damage induced p^{un} HRR deletion for each *p53* genotype.

		TOTAL	
Genotype	RPE	Eyespots	Cells
Wildtype $p^{un/un}$	34	354	652
$p53^{neo/neo}$ $p^{un/un}$	2	20	41
$p53^{R172P/R172P}$ $p^{un/un}$	8	63	118
$p53^{R172H/R172H}$ $p^{un/un}$	16	165	294

Table 2: Table of plugged female mice that have been irradiated at day 12.5. Eyes are harvested from pups born at day P30.

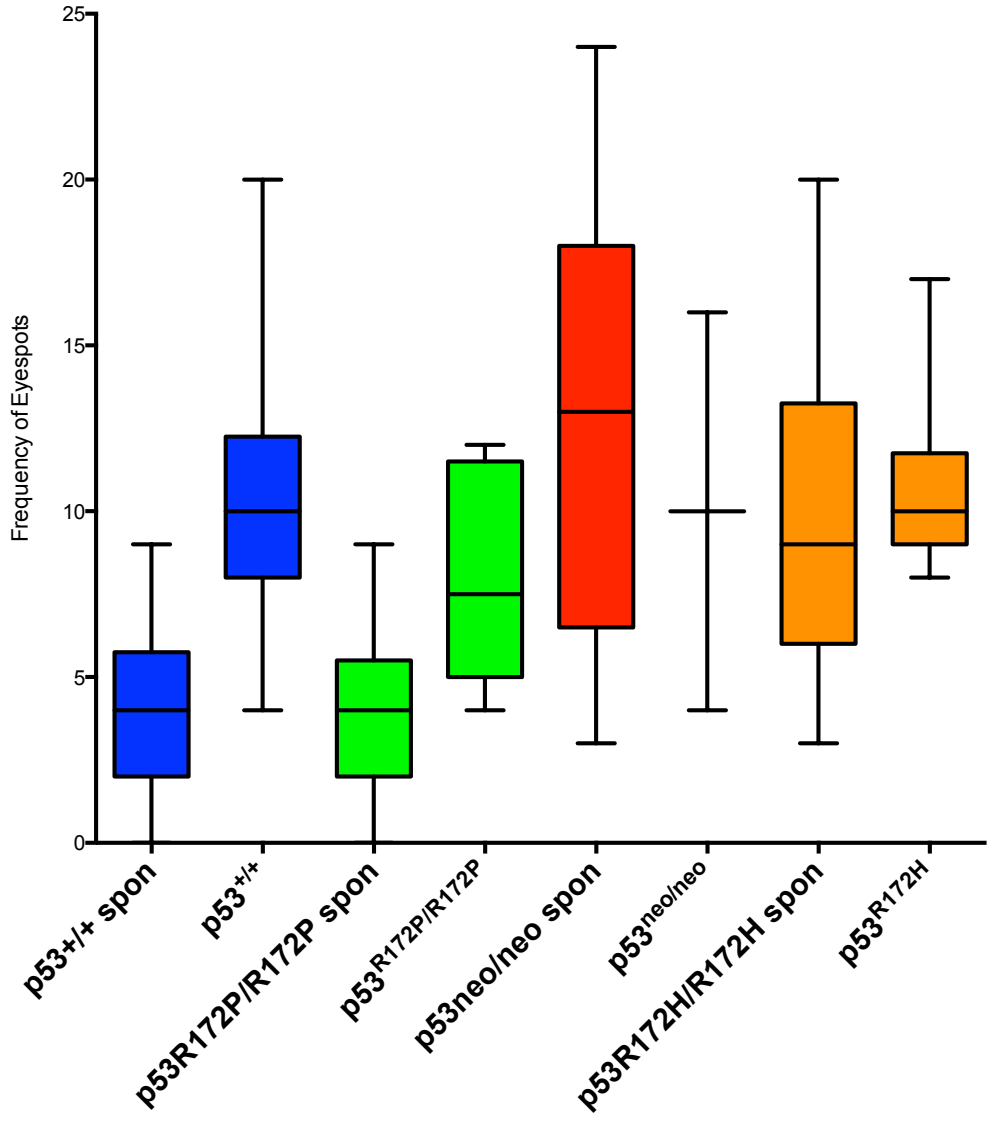

Figure 5: Figure of eyespot frequency following 1GY of X-ray in p53 WT, P53 mutant and p53 null mice compared with spontaneous.

In addition to looking at pun reversion (HR) in p53 mutant mice, we looked at the role of other lesions that may elicit an HR response. Much of the chemotherapy agents as well as environmental factors induce different lesions depending on their mode of action. We wanted to determine if these lesion could show a response in our pun reversion system.

Environmental exposures include many potential mutagens and carcinogens. Considering the variety of these agents, they are generally classified by their mode of action (17369606). Irrespective of how they react with DNA, a DNA lesion that impacts DNA replication may potentially instigate genomic instability via aberrant repair processes, including homologous recombination (HR). HR is usually considered to be a high fidelity DNA repair process, using a homologous template of DNA to repair damaged DNA. Therefore it is not surprising that it is most prevalent during or just after DNA synthesis when the sister chromatid is present to act as that template and facilitate this type of repair (21647941). However, there is also the potential that an HR event will be mediated by an alternate homologous sequence at some ectopic site, for example between simple repeats present in the genome (SINES or LINEs, segmental duplications, copy number variants, or even genes that share significant homology) (20308096). Considering that copy number variations are now understood to constitute approximately 12% (17122850) of the mammalian genome, increasing the frequency of HR by increasing exposure to DNA damaging agents might be expected to significantly impact genome stability in a proliferating somatic cell. To begin to understand the impact of such exposure on somatic genomic stability we asked what are the consequences on genome stability of exposure to several differently acting DNA damaging agents. To assess genome rearrangement we used the well-established segmental duplication/deletion pigmentation assay, the pink-eyed unstable mouse model, with *in utero* exposures to several different agents.

The pink-eyed unstable (p^{un}) mutation in the mouse is a head-to-tail duplication of a 70 kb region of DNA, effectively a segmental duplication, which disrupts the function of the *p* gene. The *p* gene encodes for an integral membrane protein that is required for the proper assembly of melanin in melanosomes conferring a dark brown/black pigmentation (7991586). The p^{un} mutation causes a dilution of this color in two pigmented cells of the mouse: melanocytes that confer coat color to fur and in the retinal pigment epithelium (RPE) of the eye. Spontaneous reversion of the 70 kb duplication via deletion of one copy of the duplicated sequence renders a functional *p* gene thus allowing for proper melanin packing in cells. These reversion events can be scored as black spots on the dilute coat or pigmented cells in the RPE of the mouse eye (14769959). Proliferation of these

tissues occurs mainly during embryonic development, thus we can expose pregnant dams to various agents during development and determine the impact on somatic HR using this simple pigment-based assay system (11285201, 11106796, 9114032, 7985029). For this study we examine the effect of six differently acting agents.

Although, first synthesized in the 1800s, the biological properties of cisplatin were discovered through a fortuitous accident 40 years ago and it has since had a major impact on the treatment of testicular and ovarian cancers. Cisplatin works by the aquation of a chloride ligand that results in the formation of a DNA adduct, usually crosslinking the DNA, which impedes replication and transcription (54213).

Alkylating agents were first developed for chemical warfare in the form of nitrogen mustard and mustard gas before being used as chemotherapeutic agents. Many of the naturally occurring alkylating agents come from plants, namely lactones (i.e. penicillin G), Methylazoxymethanolglycosides (Cycasin, macrozamin) and Nitrosamines (Dimethylnitrosamine, N-nitrosomethylurea)(5330097). Fundamentally, an alkylation reaction is either the replacement of a hydrogen atom or an addition reaction by an alkyl group. The alkylating agents methyl methanesulfonate (MMS) and ethyl methanesulfonate (EMS) are not natural products, but have been produced for use as a chemical catalyst, chemosterilants or for experimental research. Although not used as frequently in the clinic as chemotherapeutic agents, they are considered cytotoxic, mutagenic and carcinogenic and prototypical for other clinically relevant alkylating agents (8354183).

Bleomycin is a naturally occurring glycopeptide antibiotic produced by the *Streptomyces verticillus* bacterium. It has been classified as an “antitumor antibiotic.” It was originally found to have anticancer properties in a screen and has been used in the treatment of Hodgkin’s and non-Hodgkin’s lymphoma, testicular cancer and melanoma to name a few. Bleomycin acts by forming complexes with iron, which reduces molecular oxygen to superoxide and hydroxyl radicals, which in turn cause single- and double-strand breaks in DNA. As such, bleomycin is considered to be a radiomimetic (8781578).

Recent findings have shed light on the powerful potential of poly (ADP-ribose) polymerase (PARP) inhibitors to act as anticancer drugs. A first generation PARP inhibitor, 3-aminobenzamide (3AB), acts by attacking the catalytic site of PARP, thereby competing with NAD^+ and resulting in the inhibition of the activity of PARP (6248035). Third generation PARP inhibitors have been used in a pre-clinical setting based on the synthetic lethality approach to treat tumors with HR defects (15829966, 15829967, 19846859).

Etoposide is a semi-synthetic podophyllotoxin that has been used in combination chemotherapy regimens since the early 1970s. Sometimes more appropriately termed a

topoisomerase poison, etoposide acts by disrupting the normal functionality of the ubiquitous topoisomerase II enzyme that plays a role in cutting DNA strands in order to relieve tangles and supercoiling. Rather than binding or intercalating with DNA directly, etoposide stabilizes a ternary complex of topoisomerase II covalently linked to DNA at a strand break [9748545). This, in turn, prevents the subsequent religation step leading to mutational events in mammalian cells, including aneuploidy, point mutations, and chromosomal deletions and exchanges.

In this paper we sought to determine if *in utero* exposure to different classes of DNA damaging agents cause lesions that elicit HR in our pink-eyed unstable mouse model. We observed a robust induction of HR following cisplatin and alkylating agent exposure as well as a significant induction of HR following exposure to etoposide, bleomycin and the PARP inhibitor, 3AB.

Mouse cohort and breeding

C57BL/6J $p^{un/un}$ mice were obtained from the Jackson Laboratory (Bar Harbor, ME). Experimental cohorts were maintained by breeding homozygous $p^{un/un}$ mice to generate sufficient numbers of animals for exposure experiments. All animal studies were conducted in accordance with University and Institute IACUC policies, as outlined in protocol 05054-34-01-A.

Timing of pregnancy and exposure to agents

Timed matings were arranged between mice homozygous for $p^{un/un}$ with successful copulation indicated by a vaginal plug and marked as 0.5 days *post coitum*. Pregnant dams were exposed to the various agents outlined below on embryo day 12.5.

The DNA damaging agents were prepared in 0.9% normal saline (also used as a control) and given *intraperitoneally* to pregnant dams. The dose of each agent was calculated based on the weight of the pregnant dam so as not to inject more than 0.2 mL of solution per 30 g of mouse.

Agent	Mode of Action	CAS No.
Control (0.9% Normal Saline)		7647-14-5
cis-Diamineplatinum(II) dichloride	Crosslinking Agent	15663-27
Methyl methanesulfonate	Alkylating Agents	66-27-3
Ethyl Methanesulfonate		62-50-0
Bleomycin sulfate	Radiomimetic Agent	9041-93-4
3-Aminobenzamide	Parp Inhibitor	3544-24-9
Etoposide	Topoisomerase II inhibitor	33419-42-0

Table 3: Summary of different classes of reagents purchased from Sigma (St. Louis, MO) and administered *intraperitoneally* on embryo day 12.5 to pregnant dams.

Eye dissection and p^{un} reversion (homologous recombination) assay

Eyes from thirty-day old pups derived from exposed pregnant dams were harvested and dissected as previously described (11285201). Retinal pigment epithelium (RPE) whole mounts were prepared and imaged using a Zeiss Lumar version 12 stereomicroscope, Zeiss AxioVision MRm camera, and Zeiss AxioVision 4.6 software (Thornwood, NY). For each RPE, the total number of pigmented eyespots was scored along with the number of cells that comprised each eyespot as detailed in Claybon *et al.* (20660013). The position of each pigmented eyespot was also recorded to confirm the correlation between the time of exposure and the location of any induced reversion events as previously described (11106796). The criterion for scoring a p^{un} reversion event as well as the analysis of its position on the RPE was also previously outlined in Bishop *et al.* (11285201). Briefly, an eyespot is scored as one or more reverted cell (indicated by black pigmentation in an otherwise transparent cell layer) separated by no more than one unpigmented cell.

Statistics

Statistical analysis was performed using GraphPad Prism (La Jolla, CA) software. To determine statistical significance for p^{un} reversion frequency we used a nonparametric one-way analysis of variance (Kruskal-Wallis test) with the addition of a multiple comparisons test (Dunn's test). Eyespot position data was analyzed using a two-tailed unpaired t test in regions highlighted in figure 2.

Exposure to DNA damaging agents with different modes of action induces homologous recombination

Much of our understanding of HR and the development of the working models for HR processes were derived from studying the repair of induced double strand breaks. Therefore, we set out to ask whether other types of DNA lesions could induce somatic HR *in vivo*. We exposed pregnant dams at a specific time in embryo development (12.5 dpc) to DNA damaging agents that have differing modes of action. The easiest assessment of the effect of these agents is to determine the frequency of reversion events in each RPE for each agent exposure. Upon examining the frequency of eyespots (p^{un} reversions) per RPE we found that all agents, regardless of their mode of action, significantly induced HR compared to the control (Figure 6 and Table 4). A non-parametric Kruskal-Wallis test was used to determine significance followed by a Dunn's multiple comparison test. The crosslinking agent, cisplatin and both alkylating agents, MMS and EMS showed a two-fold induction of eyespots per RPE (p=0.001). There was also an increase in revertant cells (cells per RPE) for all agents compared to control (Table 4). Although not as robust, bleomycin, PARP inhibition and the topoisomerase poison, etoposide also significantly induced HR in comparison to the control (p=0.05) (Figure 6 and Table 4). This result suggests that many forms of damage, not limited to strand breaks, are capable of inducing recombinogenic lesions.

		TOTAL			AVERAGE		
Agent	**Dose**	**RPE**	**Eyespots**	**Cells**	**Eyespots per RPE**	**Cells per RPE**	**Cells per Eyespot**
Control	Saline	26	104	203	4.0 ± 1.1	7.8 ± 4.0	2.0 ± 1.3
Cisplatin	2.5 mg/kg	16	140	404	8.8 ± 3.2	25.3 ± 22.5	2.9 ± 4.4
MMS	0.2 mg/kg	15	123	290	8.2 ± 3.6	19.3 ± 14.2	2.4 ± 2.9
EMS	100 mg/kg	17	133	281	7.8 ± 2.6	16.5 ± 9.6	2.1 ± 2.2
Bleomycin	5.0 mg/kg	17	106	274	6.2 ± 3.0	16.1 ± 15.7	2.6 ± 3.4
3AB	400 mg/kg	17	104	215	6.1 ± 2.6	12.6 ± 9.6	2.1 ± 2.0
Etoposide	2.5 mg/kg	16	97	255	6.1 ± 2.4	15.9 ± 10.5	2.6 ± 3.5

Table 4: Summary of p^{un} reversion events and RPE examined following a saline control and various DNA damaging agents

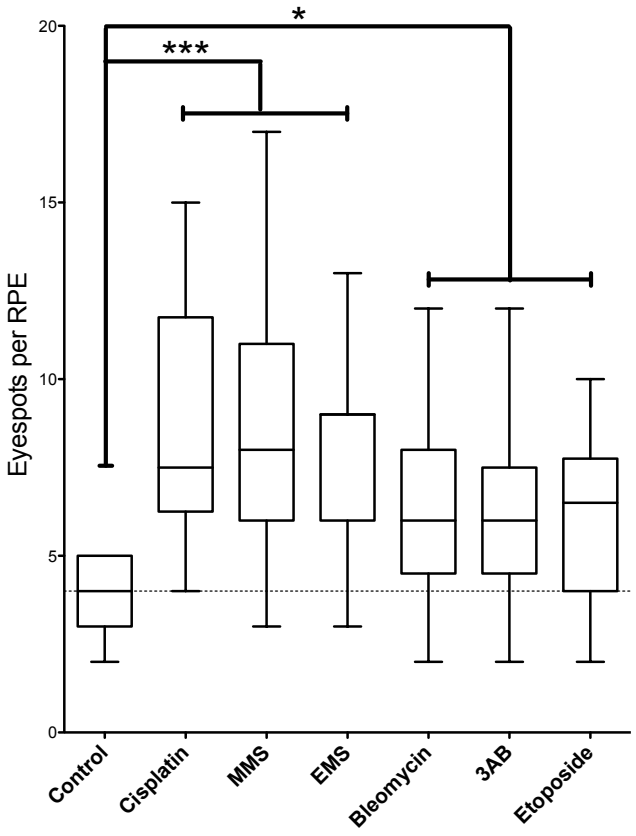

Figure 6: Box and whiskers plot of the frequency of p^{un} reversion events per RPE following saline control and DNA damaging agents. The dashed line indicates control frequency for comparison. A non-parametric Kruskal-Wallis test was used to analyze frequency data; significance is denoted by an asterisk (* p=0.05; *** p=0.001).

Position frequency of reversion events following exposure to DNA damaging agents.

RPE development results from an edge-biased pattern of proliferating cells that orient radially outward (3569658). Previously, *Bishop et al.* demonstrated that the time of exposure during development to a DNA damaging agent correlates strongly with the location of induced revertant events in the adult RPE. Therefore, those eyespots that are near to the centrally located optic nerve occur early in development, whereas those positioned towards the edge of the RPE most likely occur later in embryo development. Considering that all of the exposures were conducted at embryo day 12.5, we expect this to correlate to an induction of p^{un} reversion events at approximately one third of the distance from the optic nerve head to the edge of the RPE; “position 0.3”.

To determine if there was a positional effect of the observed increase in eyespots upon exposure to DNA damaging agents we analyzed the frequency of p^{un} reversion events in regions distal to position 0.3 on the RPE. We used t test analysis to evaluate the distribution of spot frequency for various regions between the control and RPE exposed to DNA damaging agents (regions highlighted in Figure 2a). Altogether, all classes of DNA damaging agents showed a statistically significant increase in spot frequency within the region 0.3 - 0.9 following induction of damage compared to the control.

Induction of single-cell and multi-cell reversion events differ depending on the mode of action of DNA damaging agents

In addition to directly providing HR frequency and positional timing information in a developing mouse RPE, the p^{un} reversion assay allows for the further subdivision of eyespot frequency into those eyespots consisting of one cell (single-cell eyespot) and those with more than one cell (multi-cell eyespot). The premise being that events resulting in multi-cell eyespots were most likely replication-tied, such that reversion in one cell is propagated into subsequent generations causing a clonal expansion of this event. Thus, according to our criteria we would score a clonally expanded multi-cell eyespot as a single reversion event. In contrast, a single-cell eyespot may have been derived from an event that was not tied to replication or in a cell that did not subsequently divide. Previous work with BRCA1 and BRCA2 deficient models (21709021, *data not shown*, respectively) which only retain single cell eyespots suggest that these single cell events may result from single-strand annealing (SSA), a RAD51-independent pathway that does not necessarily have to be tied with DNA replication. Examination of RPE for only single-cell eyespots revealed that all classes of DNA damaging agents showed a statistically significant increase in position frequency (region 0.3 - 0.9) compared to the control (Figure 7). Analysis of those eyespots containing more than one reverted cell (multi-cell eyespot) showed that only cisplatin (region 0.5 – 0.7), 3AB (region 0.4 – 0.8) and etoposide (region 0.5 – 0.7) significantly increased position frequency compared to control (Figure 7). In addition, the region of significance for these multi-cell events was slightly more distal from the optic nerve head than the single-cell reversion events. The difference in position between single and multi cell events was previously reported for both different genetic backgrounds (14500365) as well as following DNA damage exposure (11106796, 11285201). These results suggest a significant difference in the response/repair of different types of lesions resulting from exposure to different types of agents, with alkylating agents and the radiomimetic bleomycin inducing HR events that do not appear to be tied to replication.

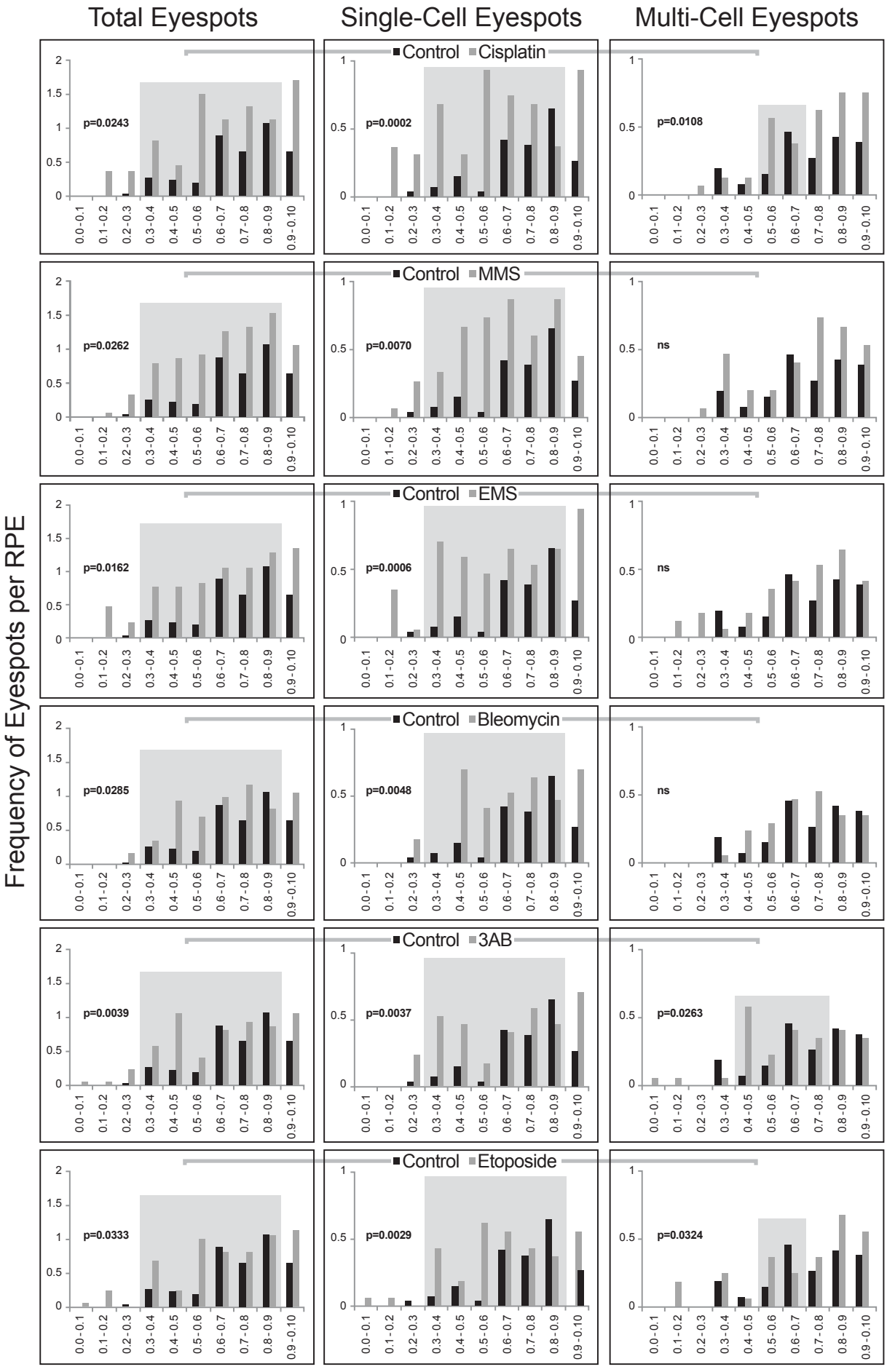
Total Eyespots
Single-Cell Eyespots
Multi-Cell Eyespots
Control Cisplatin
p=0.0243
p=0.0002
p=0.0108
Control MMS
p=0.0262
p=0.0070
ns
Control EMS
p=0.0162
p=0.0006
ns
Control Bleomycin
p=0.0285
p=0.0048
ns
Control 3AB
p=0.0039
p=0.0037
p=0.0263
Control Etoposide
p=0.0333
p=0.0029
p=0.0324
Frequency of Eyespots per RPE
Position Interval
0.0-0.1
0.1-0.2
0.2-0.3
0.3-0.4
0.4-0.5
0.5-0.6
0.6-0.7
0.7-0.8
0.8-0.9
0.9-0.10

Figure 7: Position Analysis of Total (a), Single-cell (b) and Multi-cell (c) reversion events per RPE. Position intervals are indicated on the x-axis, where 0.0 corresponds to the region near the optic nerve and 1.0 represents the edge of the RPE. Shaded boxes represent the regions of significance compared to a saline control as analyzed by an unpaired t test (p values are indicated in each box, ns= not significant).

Exposure to environmental genotoxins or endogenous byproducts of normal cellular processes represents a peril to genomic integrity. Given this, many species have adapted a robust DNA damage response program that surveys and directs appropriate repair of damaged genetic material, including single-strand and double-strand breaks, modified bases and abnormal DNA structures. In this study, we sought to determine if previously established DNA damaging agents, either naturally occurring or manufactured, were able to elicit deletion events at a particular locus by using the *in vivo* p^{un} mouse model. By determining the frequency of pigmented cell spots in the RPE we demonstrated that *in utero* exposure of these agents at an established time in embryo development resulted in an increased frequency of reversion events in our system compared to a saline control.

The cytoplasm of a wild-type RPE cell is packed with melanosomes (specialized organelles filled with melanin granules), which give these light sensitive-cells their dark guise. The murine pink-eyed dilution gene, *p*, (also called the *OCA2* gene) encodes for the P protein, which is involved in maintaining proper pH balance necessary for melanin production (11310796). When the *p* gene is nonfunctional (as in the $p^{un/un}$ genotype) melanin production is compromised resulting in a dilute color compared to the normal robust black/brown pigmentation in the RPE and other pigmented tissues such as the fur. In the event of an HR reversion of the disrupting 70kb duplication segment, a pigmented eyespot can be visualized amongst a dilute background.

The crosslinking agent cisplatin, was a strong inducer of HR in our study for the dose that was used. An increase in positional frequency in single-cell eyespots suggests the initiation of replication-independent HR mechanisms such as SSA. SSA mediates intrachromosomal deletions between homologous DNA sequences most likely caused by DSBs rather than a break induced collapsed replication fork (9804892, 9649517). In addition, eyespot size data revealed a difference in position frequency in multi-cell eyespots induced in intervals corresponding to a time later in development. This delay is likely due to the necessary time involved in converting the resultant SSB into a recombinogenic lesion (DSBs) in a proliferating cell. The mode of action of cisplatin, the aquation of the chloride ligand and subsequent crosslinking, makes proliferating cells vulnerable to DNA damage.

Once this damage is detected, DNA repair machinery (such as HR) is initiated which soon elicits an apoptotic response leading to the most likely cause of death in cancer cells. The fact that we saw an increase in single and multi-cell eyespots Cisplatin has been shown to increase SCEs in lymphocytes from control and BRCA1 mutant patients (14644329). Furthermore, *Hanneman et al.* showed increased gene conversion in meiotic stage cells upon exposure to cisplatin in the lacZ recombo mouse model based upon two differentially defective lacZ (bacterial fl-galactosidase) reporter genes under the regulatory control of a spermatogenesis-specific promoter [7514731, 9373154]. These studies involving replication-tied RAD51-dependent scenarios corroborate the increase in multi-cell events we see in this study. Cisplatin is a story of chemistry hidden in the science of biology, with its discovery and mode of action cisplatin treatment has been very effective in treating many cancers and specifically solid malignancies such as in testicular cancer.

MMS has been shown to cause tumors of the nervous system and an increased incidence of lung tumors and lymphomas have been reported after oral administration (IARC 1974). Both MMS and EMS are S(N)2 agents involved in base N-methylation that can lead to the formation of apurinic sites that block replication (15162018). Point mutations are common and typically due to guanine alkylation as well as DNA strand breaks and DNA fragmentation. The fact that these agents induce homologous recombination has been indicated by an increase in SCEs in various murine tissues including bone marrow, liver, and kidney as well as in blood and spleen lymphocytes following intraperitoneal injection of MMS (2572066). The frequency of HR was also examined using recombination between two tandemly arranged *neo* gene fragments in Chinese hamster ovary cells (CHO:5), and this frequency was found to be increased by methyl methanesulfonate (MMS) treatment (2716763). Others have also demonstrated that HR is induced by either EMS or MMS using the *in vivo* p^{un} fur-spot assay (9114032), which we now recapitulate in this paper using the more sensitive RPE eyespot p^{un} mouse model. We observed a significant increase in single-cell eyespots, however this increase was not evident in eyespots consisting of more than one cell. This suggests that alkylating agents have robust initial activity (laboratory rats injected with 100mg/kg of MMS showed no plasma levels of drug after 2 hours IARC 1974) possibly most likely leading to replication arrest or programmed cell death. Alkylating chemotherapy drugs have their effect in every phase of the cell cycle, and are thus desirable for use on a wide range of cancers. They have been shown to be very effective in the treatment of slow-growing cancers, like solid tumors and leukemia, but are also used to treat lung cancer, ovarian cancer, breast cancer and others.

Bleomycin, a DNA-cleaving agent, has been shown to induce SCEs in CHO cells in G1 (7513811) and also results in an increased frequency of HR in our *in vivo* RPE p^{un} assay. Bleomycin and the other enediyne antibiotics achieve site-specific free radical attack on sugar moieties in both

strands of DNA that can result in double-strand breaks (8781578). A similar phenomenon of robust induction of HR reversion events in more central regions of the RPE, and more specifically in single-cell eyespots, was also seen in a paper by *Bishop et al* using the p^{un} eyespot assay with X-ray damage (11106796).

3AB, being neither mutagenic nor cytotoxic, is a potent inducer of SCEs in CHO cells (6832224, 7199115). Here we show that pharmacological inhibition of PARP activity can induce HR in the *in vivo* RPE p^{un} assay. This finding recapitulates the hyperrecombination phenotype seen in work done by *Claybon et a*l. in PARP1 null mice (20660013).

The lesions resulting from etoposide exposure to cells have been shown in several studies to induce recombination. For instance, etoposide treatment for four hours caused illegitimate site-specific action of V(D)J recombinase in an *hprt* plasmid based system integrated into human lymphoid CCRF-CEM cells (8822941). Recombination was further confirmed as measured by sister chromatid exchange (SCE) following etoposide exposure in Chinese hamster ovary (CHO) cells (7664276) and in cultured human lymphocytes (8692226). Furthermore, this potent topoisomerase II inhibitor has been shown to induce somatic intrachromosomal recombination in a whole mouse transgenic (pKZI) mutagenesis model in which a lacZ transgene is only expressed after a DNA inversion (10354496, 1925563). In our study we more directly demonstrate that etoposide is capable of inducing homologous recombination in the *in vivo* p^{un} assay.

This type of work is necessary to determine the mechanism of action of much of the drugs that are used today in cancer treatment. A better understanding of the mechanism by which chemotherapeutic agents use to damage DNA will lead to better insight for drug development and more tailored treatment for patients.

Key Research Accomplishments

- R172P mutant mice are able to suppress HR similar to wild type suggesting the mechanism is not due to the transactivation of apoptotic genes but through cell cycle or protein: protein interactions.
- R172H mutant mice have a decrease in HR similar to p53 null mice, which do not produce p53 protein. This suggests a protein: protein interaction defect and a possible indirect regulatory role for p53 in the regulation of HR.
- Exposure to irradiation in R172P mutant mice leads to a robust induction of HR similar to WT. In contrast the R172H mutant has lost some functionality necessary for eliciting a proper p53 response to IR damage.
- Many DNA damaging agents with differing modes of actions and resultant lesions can elicit an HR response.

Reportable outcomes:

Peer-Reviewed Publications:

- *Induction of Homologous Recombination by DNA damaging agents with differing modes of action.* Bijal Karia, Carolina Cantu, Alexander J. R. Bishop. Manuscript in preparation 2013
- A mechanistic look at Mutant P53 and Homologous Recombination. Bijal Karia, Yidong Chen, Harry Chen, Alexander J.R. Bishop. Manuscript in preparation 2013

Conclusions

The main focus of this grant was to train me for future as an independent breast cancer investigator. Using the funds from this grant this year I have attended 2 meetings related to genomic instability (Keystone Symposia), as well as the Era of Hope Meeting where I interacted with fellow DoD awardees. My attendance at these meetings allowed me to make contacts with breast cancer investigators all over the world. I was exposed to cutting-edge research that was being done in the field of breast cancer research. My poster presentation allowed for good discussion and feedback from other investigators that will help shape future experiments and thinking about breast cancer.
I have had 1 dissertation committee meeting this year (2-21-2011) in which the discussion of my progress was key. My committee gave me invaluable advice on analysis of experiments, interpretations, statistical help and time management for progression of my PHD. We have had our final meeting and I have been given the go-ahead to complete my manuscripts and begin writing my dissertation.

I continue to attend seminars twice a week to better keep up with ongoing research in many fields. This has been a great lesson in critically thinking about the work of others and how they answered questions and solved problems.

I continually meet with my mentors on a weekly basis to discuss experiment results, future experiment planning and troubleshooting strategies.

In the first year I have made significant progress. Animal models are very difficult but I have managed to learn and master mouse husbandry and now have a thriving healthy breeding colony. The cohorts mentioned in the statement of work have all been established and experiments are underway. Assays for measuring RAD51 foci, NER, BER have been learned by the PI and are currently being used in the lab.

The most significant finding that has come from the second and third year of this grant is that there is a difference between the two p53 mutants in terms of homologous recombination frequency. Given the separation of function of these two mutants we can now tease out the mechanism for how p53 suppresses homologous recombination both in a spontaneous situation and following damage. The microarray analysis showed no differential expression of HR relevant genes between the mutants as and thus our focus will be on determine what protein-protein interaction has been disrupted between the mutants that might explain the difference in HR frequency. We are currently optimizing these experiments and hope to submit a manuscript on these findings in 2013. We will also continue to gather enough RPE to complete IR induction experiments in hopes of a their first author publication.

“So what”

the significance of these initial findings is that we are closer to determining what p53 mutations are exactly doing and not doing in cells. If we can determine what main “normal” functions of p53 are altered or lost or broken in cancer cells we can develop better targets and therapies that address these issue particularly. For example if it is determined that the more aggressive R172H mutation has a broken protein: protein interaction that causes it to have hyper recombination leading to genomic instability leading to cancer than there is a chance for targeted therapy to repair this interaction in order to restore normal DNA repair function. The research that has been done in this field by previous investigators has been on in vitro plasmid based models with questionable results. Here we use an in vivo assay in a clean genetic system that provides an excellent model for determining genomic instability by way of measuring HR.

References

1. Lane DP. Cancer. p53, guardian of the genome. Nature. 1992 Jul 2;358(6381):15-6.
2. Sherr CJ. Cancer Cell Cycles. Science. 1996 Dec 6;274(5293):1672-7.
3. Taylor WR, Stark GR. Regulation of the G2/M transition by p53. Oncogene. 2001 Apr 5;20(15):1803-15.
4. Ko LJ, Prives C. p53: Puzzle and Paradigm. Genes Dev. 1996 May 1;10(9):1054-72.
5. Brown AD, Claybon AB, Bishop AJ. A conditional mouse model for measuring the frequency of homologous recombination events in vivo in the absence of essential genes. Mol Cell Biol. 2011 Sep;31(17):3593-602. Epub 2011 Jun 27.
6. Bertrand P, Rouillard D, Boulet A, Levalois C, Soussi T, Lopez BS. Increase of spontaneous intrachromosomal homologous recombination in mammalian cells expressing a mutant p53 protein. Oncogene. 1997 Mar 6;14(9):1117-22.
7. Willers H, McCarthy EE, Wu B, Wunsch H, Tang W, Taghian DG, Xia F, Powell SN. Dissociation of p53-mediated suppression of homologous recombination from G1/S cell cycle checkpoint control. Oncogene. 2000 Feb 3;19(5):632-9.
8. Akyüz N, Boehden GS, Süsse S, Rimek A, Preuss U, Scheidtmann KH, Wiesmüller L. DNA substrate dependence of p53-mediated regulation of double-strand break repair. Mol Cell Biol. 2002 Sep;22(17):6306-17.
9. Lang GA, Iwakuma T, Suh YA, Liu G, Rao VA, Parant JM, Valentin-Vega YA, Terzian T, Caldwell LC, Strong LC, El-Naggar AK, Lozano G. Gain of function of a p53 hot spot mutation in a mouse model of Li-Fraumeni syndrome. Cell. 2004 Dec 17;119(6):861-72.
10. Olive KP, Tuveson DA, Ruhe ZC, Yin B, Willis NA, Bronson RT, Crowley D, Jacks T. Mutant p53 gain of function in two mouse models of Li-Fraumeni syndrome. Cell. 2004 Dec 17;119(6):847-60.
11. Aubrecht J, Secretan MB, Bishop AJ, Schiestl RH. Involvement of p53 in X-ray induced intrachromosomal recombination in mice. Carcinogenesis. 1999 Dec;20(12):2229-36.
12. Bishop AJ, Kosaras B, Carls N, Sidman RL, Schiestl RH. Susceptibility of proliferating cells to benzo[a]pyrene-induced homologous recombination in mice. Carcinogenesis. 2001 Apr;22(4):641-9.
13. Claybon A, Karia B, Bruce C, Bishop AJ. PARP1 suppresses homologous recombination events in mice in vivo. Nucleic Acids Res. 2010 Nov;38(21):7538-45. Epub 2010 Jul 21.

14. Bishop AJ, Hollander MC, Kosaras B, Sidman RL, Fornace AJ Jr, Schiestl RH. Atm-, p53-, and Gadd45a-deficient mice show an increased frequency of homologous recombination at different stages during development. Cancer Res. 2003 Sep 1;63(17):5335-43.

Appendix-1

microarray hit list

273 genes (yy22)	known p53 target genes	matches	FC_HH_PP	direction in HH
Cdkn2a	Ccnb1	10	4.409	upregulated
Cdkn2a	Ccng1	10	4.888	upregulated
Cdkn2a	Ccng1	10	4.773	upregulated
Cdkn2a	Cd82	10	4.453	upregulated
Cdkn2a	Cdc25c	10	4.440	upregulated
Cdkn2a	Cdc25c	10	4.821	upregulated
Cdkn2a	Cdc2a	10	4.840	upregulated
Cdkn2a	Cdc2a	10	4.428	upregulated
Cdkn2a	Cdk4	10	4.722	upregulated
Cdkn2a	Cdkn1a	10	4.603	upregulated
Mmp13	Fos	1	-6.912	downregulated
Perp	Il6	1	-47.175	downregulated
Pgam2	Il6	1	-3.594	downregulated
Serpinb5	Mdm2	1	-22.723	downregulated
Srgn	Mrpl41	1	-12.622	downregulated
1190003J15Rik	1190002H23Rik	0	-8.434	downregulated
2010005H15Rik	Abcb1b	0	-10.230	downregulated
2210011C24Rik	Abcb1b	0	-4.580	downregulated
2210409E12Rik	Abcb1b	0	-9.085	downregulated
2210409E12Rik	Acta2	0	-4.603	downregulated
2310043J07Rik	Acta2	0	-7.862	downregulated
2810432L12Rik	Acta2	0	-2.901	downregulated
4933413A10Rik	Acta2	0	-5.923	downregulated
5730410E15Rik	Acta2	0	-3.963	downregulated

6330403K07Rik	Acta2	0	-7.923	downregulated
6330530A05Rik	Acta2	0	-2.944	downregulated
9130213B05Rik	Acta2	0	-3.636	downregulated
9930013L23Rik	Acta2	0	-9.753	downregulated
9930013L23Rik	Acta2	0	-9.045	downregulated
9930013L23Rik	Acta2	0	-6.153	downregulated
A_52_P1004880	Acta2	0	-6.113	downregulated
A930038C07Rik	Acta2	0	-15.082	downregulated
Aard	Acta2	0	-8.707	downregulated
Ablim3	Afp	0	-5.628	downregulated
Acss1	Afp	0	-24.660	downregulated
Actn2	Afp	0	-12.365	downregulated
Adora1	Afp	0	-11.359	downregulated
AK086961	Afp	0	-16.885	downregulated
Akap6	Afp	0	-5.967	downregulated
Akp2	Afp	0	-5.328	downregulated
Aldh1a3	Afp	0	-3.611	downregulated
Alms1	Afp	0	2.864	upregulated
Apod	Afp	0	-3.415	downregulated
Apoe	Apaf1	0	-9.794	downregulated
Apoe	Apaf1	0	-9.220	downregulated
Apoe	Apaf1	0	-9.651	downregulated
Apoe	Bai1	0	-9.603	downregulated
Apoe	Bai1	0	-9.827	downregulated
Apoe	Bax	0	-9.979	downregulated
Apoe	Bax	0	-9.860	downregulated
Apoe	Bax	0	-10.074	downregulated
Apoe	Bax	0	-9.727	downregulated

Apoe	Bax	0	-9.720	downregulated
Atp1a2	Bax	0	-18.437	downregulated
BC099439	Bax	0	-29.442	downregulated
BC117090	Bax	0	-30.091	downregulated
BC117090	Bax	0	-33.872	downregulated
BC117090	Bax	0	-30.050	downregulated
BU920841	Bbc3	0	-5.938	downregulated
BY439412	Bcl2	0	-8.238	downregulated
C1qa	Bcl2	0	-8.371	downregulated
C1qc	Bcl2	0	-5.394	downregulated
C3	Bcl2	0	-16.408	downregulated
C3	Bcl2	0	-16.677	downregulated
C3	Bcl2	0	-15.996	downregulated
C3	Bcl2	0	-15.358	downregulated
C3	Bcl2	0	-16.662	downregulated
C3	Bcl2	0	-16.520	downregulated
C3	Bcl2	0	-17.032	downregulated
C3	Bcl2	0	-16.546	downregulated
C3	Bcl2	0	-17.907	downregulated
C3	Bdkrb2	0	-17.259	downregulated
C4b	Birc5	0	-7.503	downregulated
Cacna1s	Brca1	0	-8.795	downregulated
Car2	Brca1	0	-8.964	downregulated
Casq2	Btg2	0	-10.013	downregulated
Cav3	Btg2	0	-6.843	downregulated
Cbr1	Btg2	0	-5.437	downregulated
Ccdc116	Casp1	0	3.498	upregulated
Ccl5	Casp6	0	-3.956	downregulated

Cd200	Ccnb1	0	-7.538	downregulated
Cdh13	Ccnb1	0	-3.985	downregulated
Ceacam2	Cdkn1a	0	-5.721	downregulated
Celsr1	Cdkn1a	0	-27.824	downregulated
Cfb	Cdkn1a	0	-9.096	downregulated
Cfh	Cdkn1a	0	-24.207	downregulated
Cfh	Cdkn1a	0	-8.093	downregulated
Chrna1	Cdkn1a	0	-9.927	downregulated
Chrng	Cdkn1a	0	-23.899	downregulated
Clec4d	Cdkn1a	0	-5.624	downregulated
Clu	Cdkn1a	0	-9.058	downregulated
Cma1	Cdkn2a	0	-4.766	downregulated
Cntn1	Cdkn2a	0	-4.710	downregulated
Col22a1	Cdkn2a	0	-3.901	downregulated
Col2a1	Cdkn2a	0	-17.342	downregulated
Col5a3	Cdkn2a	0	-3.302	downregulated
Col9a2	Cdkn2a	0	-3.896	downregulated
Cox8b	Cdkn2a	0	-3.560	downregulated
Cpb1	Cdkn2a	0	3.532	upregulated
Crym	Cdkn2a	0	-5.231	downregulated
Cuedc1	Cdkn2a	0	5.486	upregulated
Cuedc1	Chek1	0	4.265	upregulated
Cxcl14	Chek1	0	-3.756	downregulated
Cxcl16	Ckm	0	-3.144	downregulated
Cxcl4	Ctnnb1	0	-7.022	downregulated
Cyp26b1	Ctnnb1	0	-9.272	downregulated
Cyp51	Ctnnb1	0	3.108	upregulated
D430036J16Rik	Ctnnb1	0	4.430	upregulated

Dct	Ctnnb1	0	-97.213	downregulated
Ddit4l	Ctnnb1	0	-2.959	downregulated
Ddit4l	Ctnnb1	0	-3.368	downregulated
Ddx4	Ctnnb1	0	16.300	upregulated
Dhcr24	Ctnnb1	0	2.877	upregulated
Dio3	Ctnnb1	0	-5.421	downregulated
Dok7	Ctnnb1	0	-10.989	downregulated
Dscr1l1	Ctnnb1	0	-2.867	downregulated
EG433016	Ctsd	0	-11.387	downregulated
Elovl6	Ctsd	0	2.845	upregulated
Elovl7	Cx3cl1	0	-4.512	downregulated
Emid2	Cx3cl1	0	-14.981	downregulated
Enpp2	Dab2ip	0	-18.235	downregulated
Epha3	Ddb1	0	4.163	upregulated
Epyc	Dkk1	0	-29.371	downregulated
Esco1	Dkk1	0	2.814	upregulated
Esco1	Ecm1	0	3.853	upregulated
Expi	Ecm1	0	-8.228	downregulated
Fabp7	Eef1a1	0	-14.370	downregulated
Fmod	Eef1a1	0	-3.587	downregulated
Galntl1	Egfr	0	-3.701	downregulated
Gpr149	Egfr	0	6.196	upregulated
Gprasp2	Egfr	0	-8.921	downregulated
Gprc5c	Egfr	0	-5.598	downregulated
Gprc5c	Egfr	0	-4.395	downregulated
Gvin1	Egfr	0	2.956	upregulated
Gzmd	Egfr	0	-3.437	downregulated
H2-Q10	Egfr	0	-5.190	downregulated

Heyl	Egfr	0	-3.268	downregulated
Hist2h2bb	Egfr	0	5.161	upregulated
Hoxc5	Egfr	0	7.113	upregulated
Hoxc6	Egfr	0	3.825	upregulated
Hsd11b1	Egfr	0	-9.275	downregulated
Ica1	Egfr	0	3.844	upregulated
Id4	Egfr	0	-3.858	downregulated
Id4	Egfr	0	-2.956	downregulated
Idi1	Egfr	0	4.372	upregulated
Igf2	Egfr	0	-3.069	downregulated
Igf2	Egfr	0	-3.246	downregulated
Igf2	Egfr	0	-3.186	downregulated
Igf2	Egfr	0	-3.173	downregulated
Igf2	Egfr	0	-3.342	downregulated
Igf2	Egfr	0	-3.232	downregulated
Igf2	Egfr	0	-3.194	downregulated
Igf2	Ei24	0	-3.277	downregulated
Igf2	Fas	0	-3.153	downregulated
Igf2	Fas	0	-3.258	downregulated
Igf2	Fas	0	-3.477	downregulated
Igfbp2	Fas	0	-14.006	downregulated
Il31ra	Fas	0	7.839	upregulated
Itga4	Fas	0	4.272	upregulated
Itgav	Fas	0	3.047	upregulated
Itm2a	Fas	0	-3.216	downregulated
Krt16	Fas	0	-10.636	downregulated
Krt17	Fas	0	-6.131	downregulated
Krt5	Fas	0	-4.171	downregulated

Lcn2	Fos	0	-14.604	downregulated
Lmod3	Fos	0	-5.392	downregulated
Loxl3	Fos	0	3.522	upregulated
Lrrc33	Fos	0	-3.604	downregulated
Lrrn1	Fos	0	-8.435	downregulated
Lss	Fos	0	3.224	upregulated
Ltf	Fos	0	-12.736	downregulated
Mcpt4	Fos	0	-4.108	downregulated
Megf10	Fos	0	3.241	upregulated
Mmp3	Gadd45a	0	-78.547	downregulated
Mmp9	Gadd45b	0	-13.325	downregulated
Mmp9	Gadd45b	0	-9.667	downregulated
Mmp9	Gadd45g	0	-16.024	downregulated
Mmp9	Gdf15	0	-22.648	downregulated
Mmp9	Glipr2	0	-13.787	downregulated
Mmp9	Gml	0	-9.640	downregulated
Mmp9	Gml	0	-12.186	downregulated
Mmp9	Gpx1	0	-13.836	downregulated
Mmp9	Gpx2	0	-12.735	downregulated
Mmp9	Gpx3	0	-10.662	downregulated
Mpeg1	Gpx4	0	-3.573	downregulated
Mybph	Gpx5	0	-12.218	downregulated
Myh1	Gpx6	0	-12.705	downregulated
Myh2	Gpx7	0	-6.800	downregulated
Myh3	Gtse1	0	-17.364	downregulated
Myh3	Hbegf	0	-13.812	downregulated
Myh7	Hgf	0	-10.491	downregulated
Myh7	Hgf	0	-12.840	downregulated

Myh8	Hgf	0	-8.518	downregulated
Myl1	Hgf	0	-7.346	downregulated
Mylpf	Hic1	0	-7.148	downregulated
Myo18b	Hspa2	0	-11.816	downregulated
Myo1g	Hspa2	0	-4.548	downregulated
Myod1	Igfbp3	0	-3.889	downregulated
Myod1	Igfbp3	0	-10.346	downregulated
Myod1	Igfbp3	0	-6.056	downregulated
Myod1	Il2	0	-6.417	downregulated
Myog	Il2	0	-7.371	downregulated
Myog	Il2	0	-7.653	downregulated
Myog	Il2	0	-7.162	downregulated
Myog	Il2	0	-9.198	downregulated
Myog	Il2	0	-8.294	downregulated
Myog	Il2	0	-7.614	downregulated
Myog	Il2	0	-7.279	downregulated
Myog	Il2	0	-8.824	downregulated
Myog	Il2	0	-6.874	downregulated
Myog	Il2	0	-6.733	downregulated
Myom2	Il4	0	-6.573	downregulated
NAP102441-1	Il4	0	2.969	upregulated
NAP102683-1	Il4	0	3.033	upregulated
NAP124154-1	Il4	0	6.772	upregulated
Ncf2	Il4	0	-3.284	downregulated
Npr3	Il4	0	-4.895	downregulated
Npy	Il4	0	-7.725	downregulated
Pcsk9	Il4	0	5.072	upregulated
Pdlim3	Il4	0	-3.809	downregulated

Pdlim3	Il4	0	-4.742	downregulated
Pkp1	Il6	0	-16.815	downregulated
Plcl1	Il6	0	5.463	upregulated
Plekha6	Il6	0	-3.501	downregulated
Plxna4	Il6	0	2.969	upregulated
Prg4	Il6	0	-34.291	downregulated
Prkg2	Il6	0	4.053	upregulated
Prnd	Il6	0	-5.292	downregulated
Prss12	Il6	0	-3.582	downregulated
Prss35	Insr	0	-4.751	downregulated
Ptn	Krt8	0	6.778	upregulated
Ptx3	Krt8	0	-3.730	downregulated
Ptx3	Lrdd	0	-3.334	downregulated
Rarres2	Lrdd	0	-20.800	downregulated
Rarres2	Lrdd	0	-18.322	downregulated
Rtn1	Mdm2	0	-6.389	downregulated
S100a8	Mdm2	0	-19.926	downregulated
S100a9	Mdm2	0	-76.564	downregulated
Saa1	Mdm2	0	-8.292	downregulated
Saa3	Mdm2	0	-21.669	downregulated
Scn3b	Mdm2	0	-10.730	downregulated
Scn5a	Mdm2	0	-8.937	downregulated
Scube1	Mdm2	0	-7.061	downregulated
Serping1	Mdm2	0	-4.767	downregulated
Slc16a6	Mdm2	0	-2.974	downregulated
Slpi	Met	0	-11.207	downregulated
Snx24	Met	0	2.998	upregulated
Snx24	Met	0	4.197	upregulated

Sorbs2	Mmp13	0	-3.926	downregulated
Sparcl1	Mmp1a	0	-29.972	downregulated
Sparcl1	Mmp1a	0	-31.026	downregulated
Spon1	Mmp2	0	-15.063	downregulated
St6galnac2	Mrpl41	0	-2.828	downregulated
Stard4	Mtap4	0	3.218	upregulated
TC1651696	Mtap4	0	-4.156	downregulated
Thy1	Mtap4	0	2.995	upregulated
Tmem182	Mtap4	0	-7.618	downregulated
Tmem30b	Mtap4	0	-3.751	downregulated
Tnni1	Myc	0	-11.236	downregulated
Tnni1	Myc	0	-7.908	downregulated
Tnnt1	Myc	0	-4.720	downregulated
Trem2	Myc	0	-4.088	downregulated
Trf	Myc	0	-4.752	downregulated
Trim63	Myc	0	-4.120	downregulated
U90926	Myc	0	-9.384	downregulated
Unc13a	Myc	0	3.168	upregulated
Unc5b	Myc	0	3.386	upregulated
Vcan	Myc	0	3.371	upregulated
Wars2	Myc	0	3.432	upregulated
Wdr40b	Myc	0	-3.155	downregulated
Wnt10a	Ndrg1	0	-12.063	downregulated
Zfp185	Nos3	0	-5.004	downregulated
Zfp318	Nos3	0	-5.097	downregulated
	Nos3			
	Nos3			
	Nos3			

Nos3

Nos3

Nos3

Nos3

Nos3

P2rxl1

P2rxl1

Pcbp4

Pcna

Pcna

Pcna

Pcna

Pcna

Pcna

Pcna

Pcna

Pcna

Pcna

Pcna

Perp

Pgam2

Plagl1

Plagl1

Pmaip1

Pold1

Pold1

Polk

Polk

Ppm1d

Ppm1d